JOURNAL OF GEOPHYSICAL RESEARCH, VOL. 101, NO. C10, PAGES 25,575–25,587, NOVEMBER 15, 1996

# Observations and predictions of run-up

B. Raubenheimer and R. T. Guza

Scripps Institution of Oceanography, University of California, San Diego

**Abstract.** For a significant range of offshore wave conditions and foreshore slopes, run-up observations are compared to semiempirical formulations and predictions of an existing numerical model based on the depth-averaged one-dimensional nonlinear shallow water equations with bore-like breaking wave dissipation and quadratic bottom friction. The numerical model is initialized with time series of sea surface elevation and cross-shore velocity observed in 80 cm mean water depth (approximately 50 m offshore of the mean shoreline) on a gently sloping beach and in 175 cm water depth (100 m offshore of the shoreline) on a steep concave beach. Run-up was measured with a stack of resistance wires at elevations 5, 10, 15, 20, and 25 cm above and parallel to the beach face. At sea swell frequencies (nominally $0.05 < f \leq 0.18$ Hz), run-up energy is limited by surf zone dissipation of shoreward propagating waves so that increasing the offshore wave height above a threshold value does not substantially increase the predicted or observed sea swell run-up excursions (e.g., run-up is "saturated"). Existing semiempirical saturation formulations are most consistent with the observations and numerical model predictions of run-up excursions nearest the bed. In contrast, at infragravity frequencies ($0.004 < f \leq 0.05$ Hz) where surf zone dissipation is relatively weak and reflection from the beach face is strong (e.g., saturation formulas are not applicable), the run-up excursions increase approximately linearly with increasing offshore wave height. The numerical model also accurately predicts that the tongue-like shape of the run-up results in sensitivity of run-up measurements to wire elevation. For instance, run-up excursions and mean vertical superelevation (above the offshore still water level) increase with decreasing wire elevation, and continuous thinning of the run-up tongue during the wave uprush can result in large phase differences between run-up excursions measured at different wire elevations. Numerical model simulations suggest that run-up measured more than a few centimeters above the bed cannot be used to infer even the sign of the fluid velocities in the run-up tongue.

## 1. Introduction

On the basis of laboratory observations of breaking monochromatic waves on a planar beach, *Miche* [1951] hypothesized that run-up, loosely defined as the time-varying location of the shoreward edge of the water on the beach face, can be saturated (i.e., independent of the offshore wave height). Shoreward propagating wave energy exceeding a threshold value is assumed dissipated by wave breaking within the surf zone, so run-up oscillations do not increase in magnitude above a limit which depends on the wave frequency and beach slope. The shoreward propagating energy which is not dissipated is assumed to reflect from the beach face and form standing waves. *Carrier and Greenspan* [1958] showed analytically that on a planar beach, a monochromatic standing wave solution (e.g., nonbreaking) to the inviscid nonlinear shallow water equations exists when

$$\epsilon_s = \frac{a_s \omega^2}{g \tan^2 \beta} \leq 1 \tag{1}$$

where $\epsilon_s$ is a nondimensional constant, $a_s$ is the vertical swash amplitude at the shoreline, $\omega$ is the primary wave frequency ($f$) in radians, $g$ is gravitational acceleration, and $\beta$ is the beach slope. Combining Miche's saturation hypothesis with (1) to determine the maximum run-up amplitude, using linear theory to relate wave amplitudes at the shoreline and deep water, and assuming a gentle beach slope ($\tan\beta \approx \beta$), the vertical run-up height, $R_v$, normalized by the deep water wave height of the shoreward propagating wave, $H_0$, is given by

$$\frac{R_v}{H_0} = \begin{cases} \left(\frac{\pi}{2\beta}\right)^{1/2} & : \xi_0 \geq \xi_c \quad : \text{reflective} \\ \frac{\xi_0^2}{\pi} & : \xi_0 < \xi_c \quad : \text{saturated} \end{cases} \tag{2}$$

where $\xi_0 = \beta/\sqrt{H_0/L_0}$ is the Irribarren number, $L_0$ is the deep water wavelength, and $\xi_c = |\pi^3/2\beta|^{1/4}$. Note that when the run-up is saturated (2), $R_v$ is indepen-



Paper number 96JC02432.
0148-0227/96/96JC-02432$09.00

dent of $H_0$. Alternatively, on the basis of laboratory observations of monochromatic wave run-up, *Hunt* [1959] proposed a linear dependence, in engineering practice known as "Hunt's Formula," between normalized run-up and $\xi_0$:

$$\frac{R_v}{H_0} = \xi_0. \tag{3}$$

Assuming saturation and unattenuated propagation of the seaward going reflected wave, the squared reflection coefficient, $Re^2$ (defined as the ratio of seaward to shoreward propagating energy), outside the surf zone is approximately (from (2, $\xi_0 < \xi_c$))

$$Re^2_{\text{deep}} \approx \begin{cases} 1 & : \quad \xi_0 \geq \xi_c \\ M & : \quad \xi_0 < \xi_c \end{cases} \tag{4}$$

where $M = (16g^2\beta^5)/(2\pi H_0^2\omega^4) = (\xi_0/\xi_c)^4$. Studies of the run-up and reflection of monochromatic waves show qualitative agreement with (1) - (4) (and with slightly modified versions of them) [*Moraes*, 1970; *Battjes*, 1974; *Guza and Bowen*, 1976; *Kobayashi and Watson*, 1987; *Kobayashi et al.*, 1987, 1988].

It is unclear how to extend the above semiempirical results for monochromatic waves to random waves. In analogy to (1), *Huntley et al.* [1977] suggested that the saturated vertical run-up spectrum for random waves, $R_v^2(\omega)$, is given by

$$R_v^2(\omega) = \epsilon^2 g^2 \beta^4 \omega^{-4}. \tag{5}$$

where $\epsilon$ is a dimensional constant (units $\mathrm{Hz}^{-1/2}$) perhaps related to the bandwidth of the saturated spectrum. The gross features of the Miche saturation hypothesis, extended to random waves, have been qualitatively verified. Consistent with (5), laboratory observations on planar beaches showed that spectral levels of random wave run-up at sea swell frequencies vary approximately as $\beta^4$ and $\omega^{-4}$ [*Sawaragi and Iwata*, 1984; *Mase*, 1988]. Furthermore, comparisons of field measurements to (2, $\xi_0 < \xi_c$) (with $H_0$ approximated by the offshore significant (defined as $4\sigma$ where $\sigma^2$ is the total variance) wave height, $H_s$, $L_0$ approximated by the deep water wavelength at either the peak or centroidal frequency, and $\beta$ approximated by the foreshore slope) and (5) suggested that run-up on ocean beaches is often saturated at sea swell frequencies [*Huntley et al.*, 1977; *Guza and Thornton*, 1982; *Guza et al.*, 1984; *Mizugushi*, 1984]. In other studies, wave run-up observations are consistent with a form of Hunt's Formula (3) modified for random waves [e.g., *Van Oorschot and d'Agremond*, 1968; *Ahrens*, 1981; *Holman and Sallenger*, 1985]. *Elgar et al.* [1994] showed that in 13 m depth the "bulk" squared reflection coefficient (i.e., based on the seaward and shoreward propagating energy integrated over the sea swell frequency band, nominally 0.05-0.20 Hz) is roughly consistent with (4), where $\xi_0$ is based on the sea swell band-integrated significant wave height and centroidal frequency (see also *Tatavarti et al.* [1988]).

The observations of random wave run-up qualitatively confirming Miche's saturation hypothesis differ in detail (e.g., the measured frequency dependence varies between $f^{-3}$ and $f^{-4}$), possibly owing to differences in run-up measurement techniques. *Holman and Sallenger* [1985] used video images in which the run-up location corresponds to the location of the foamy (high brightness contrast) edge of the waterline. Other data were collected with run-up wires, supported above and parallel to the beach face, which measure the most shoreward location at which the water depth equals the wire elevation. Comparisons of video- and wire-based run-up observations show that (on a moderately sloped beach with relatively low energy swash excursions) video measurements roughly correspond to data acquired with wires supported less than a few centimeters above the beach face and that, owing to thin run-up tongues, run-up wire measurements are sensitive to wire elevation [e.g., *Holland et al.*, 1995].

It has not been demonstrated that the semiempirical formulas for the run-up, (2, $\xi_0 < \xi_c$), (3), and (5), and reflection (4) of random waves are consistent with dynamical models. *Kobayashi and Wurjanto* [1992] and *Raubenheimer et al.* [1995] showed that run-up properties (including spectral shapes) observed on several natural beaches were predicted at least qualitatively well by a numerical model (hereinafter referred to as Rbreak) based on the depth-averaged nonlinear shallow water equations with bore-like dissipation and quadratic bottom friction [*Wurjanto and Kobayashi*, 1991]. In these studies the model was initialized with observations acquired in 1 to 4-m water depth, between 50 and 300 m from shore, and wave properties were predicted at shoreward locations. The complications of the natural environment did not significantly degrade the performance of Rbreak relative to that for normally incident random waves over an impermeable bed in a narrow laboratory flume [*Kobayashi et al.*, 1990; *Wise et al.*, 1991; *Cox et al.*, 1992]. However, the conditions for model initialization were only approximately known in the model-field data comparisons of *Kobayashi and Wurjanto* [1992]. The range of beach slopes and offshore wave heights considered by *Raubenheimer et al.* [1995] was too small to determine whether the observations and Rbreak model predictions are consistent with saturation formulas. In the present work, a larger data set is used to further validate Rbreak and to show that both the observations and Rbreak model predictions in the sea swell frequency band are qualitatively consistent with semiempirical saturation expressions for run-up and reflection.

Consistent with previous studies [e.g., *Suhayda*, 1974] the present results suggest that infragravity waves in the surf zone are often dominated by free cross-shore standing waves that are nearly completely reflected at the shoreline. Infragravity frequency run-up energy levels fall below the $f^{-4}$ levels of the sea swell band (e.g., are unsaturated) and therefore cannot be predicted by saturation models. Rbreak (initialized in 1 to 3-m water depth) accurately predicts run-up in the infragravity frequency band.

Detailed field observations of the shape of the run-up tongue and the fluid velocities within the tongue are very sparse, owing to the difficulty of obtaining accurate measurements in this relatively thin, high-velocity, sediment-laden fluid layer. Rbreak results suggest that run-up tongues thin owing to mass conservation and fluid velocities which are largest at the run-up tip. Continuous thinning of the run-up tongue during wave uprush sometimes results in offshore directed run-up measured (and predicted) at 25 cm above the bed, while near-bed run-up and velocities within the run-up tongue are directed onshore.

The observations and numerical model are briefly discussed in sections 2 and 3, respectively. Model-data comparisons are presented in section 4, followed by a discussion and conclusions.

## 2. Observations

Pressure and current fluctuations within the surf zone and run-up were measured at two sites in southern California. In both experiments, run-up was measured with five resistance wires, stacked vertically with the bottom wire 5 cm above and parallel to the bed and 5 cm separation between wires. Each run-up wire measures the most shoreward location where the water depth equals the wire elevation. Horizontal run-up locations were converted to vertical elevations using the beach profile and the wire elevation (e.g., Figure 1c). Beach profiles, measured daily, varied little (typically < 10 cm) during the experiments. Foreshore slopes, calculated over the section of beach face spanned by a typical swash excursion (about 20-m width), changed by less than 0.004 at any location.

In June 1989, a pressure sensor and an electromagnetic current meter were collocated in about 80-cm water depth on the fine-grained (mean sediment diameter about 0.2 mm) Scripps Beach, about 50 m offshore of the mean shoreline (Figure 1a). Beach slopes in the swash region (measured daily) ranged from 0.02 to 0.05 depending on tidal stage, and the offshore slope was approximately 0.01. Offshore significant wave heights measured in approximately 7-m depth ranged from 50 to 82 cm and peak frequencies were approximately 0.10 Hz. Six 68-min-long data runs were acquired at an 8-Hz sample rate over 4 days. *Holland et al.* [1995] and *Raubenheimer et al.* [1995] further describe the run-up wires and the Scripps experiment.

In October 1993, nine pressure sensors were deployed on a cross-shore transect between the shoreline and a mean water depth of 175 cm at San Onofre State Beach (Figure 1b). Current meters were collocated with the pressure sensors in mean depths of 175 and 139 cm (about 100 and 40 m offshore, respectively). Owing to the steep concave beach and tide levels that varied by as much as 2.5 m, foreshore slopes in the swash region (measured daily) ranged from 0.04 to 0.11, while the offshore slope was similar to that at Scripps (0.01). Typical grain sizes increased from about 0.1 mm at the elevation of the lowest spring tide to 0.3 mm at the berm crest. Offshore significant wave heights, measured in approximately 10-m depth a few kilometers southeast of the experiment site, ranged from 45 to 134 cm and peak frequencies ranged from 0.06 to 0.09 Hz. Considerable effort was required to keep the wires free of kelp and debris, especially during high tides when waves broke on the steep beach face. During the 10-day experiment, forty-three 68-min-long data runs were acquired at a 2-Hz sample rate.

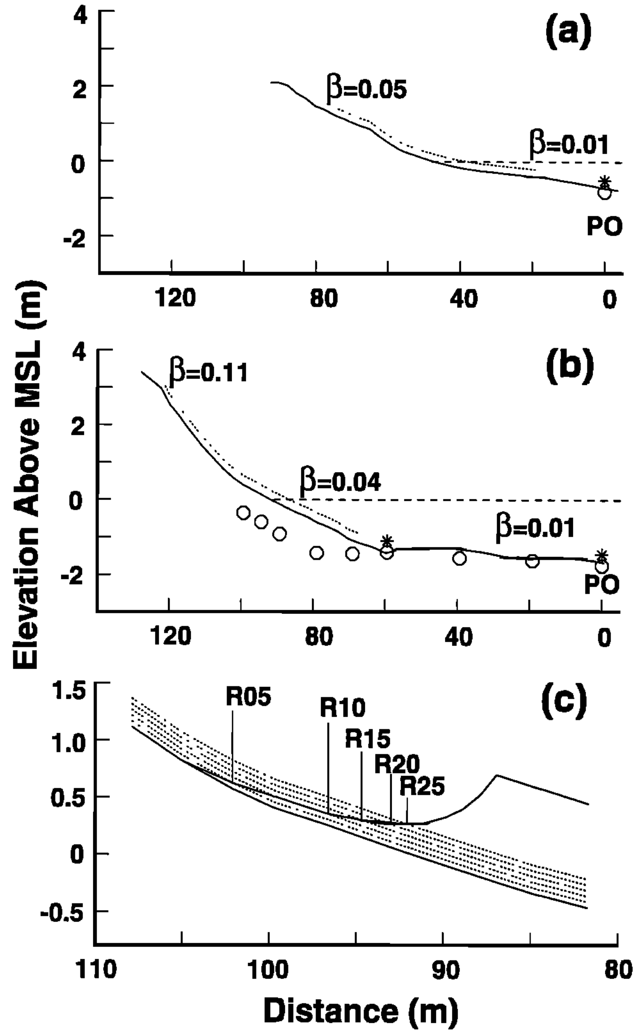


**Figure 1.** Foreshore slopes, $\beta$, and locations of pressure sensors (circles), current meters (asterisks), stacked run-up wires (dotted lines), and mean sea level (dashed line) at (a) Scripps and (b) San Onofre. (c) Schematic illustration of instantaneous run-up locations measured by each wire. The $x$ axis, positive onshore, is zero at the sensor location where the numerical model is initialized.

Data from San Onofre and Scripps were processed similarly. Sea surface elevations were estimated assuming that the measured pressure field is hydrostatic. Data runs were quadratically detrended to remove tides and other motions with periods longer than roughly 1 hour. Offshore significant wave heights (e.g., in 7 to 10-m water depth), peak frequencies, and foreshore slopes (somewhat arbitrarily defined as the slope between the Rbreak predicted maximum and minimum run-up at 5 cm above the beach face) were used to compute $\xi_0$ ((2, $\xi_0 < \xi_c$), (3), and (4)). (Similar foreshore slope estimates can be obtained by assuming a "setup" of $0.3H_s$ and a vertical swash height of $H_s$ rather than using

Rbreak predictions.) On the basis of (2, $\xi_0 < \xi_c$) the sea swell run-up excursions are expected to be saturated for $\xi_0$ less than roughly 3.4, a condition satisfied for all runs considered here.

Run-up wires will be identified by their elevation (in centimeters) above the bed (e.g., R05 and R25 are the bottom and top wires, respectively). Pressure sensors will be identified by their distance (in meters) from the most offshore pressure sensor (e.g., P0 and P100 are the offshore and onshore gages at San Onofre, respectively).

## 3. Model

Many analytical and numerical models of wave propagation in shallow water and the subsequent run-up are based on the one-dimensional depth-averaged nonlinear shallow water equations (here with quadratic friction),

$$\frac{\partial h}{\partial t} + \frac{\partial}{\partial x}(hu) = 0 \qquad (6)$$

$$\frac{\partial}{\partial t}(hu) + \frac{\partial}{\partial x}(hu^2) = -gh\frac{\partial \eta}{\partial x} - \frac{1}{2}f_c|u|u \qquad (7)$$

where $t$ is time, $x$ is the distance onshore from the model seaward boundary, $h$ is the total water depth, $\eta$ is the deviation from the still water depth, $u$ is the depth-averaged cross-shore velocity, and $f_c$ is a constant empirical friction coefficient [e.g., *Carrier and Greenspan*, 1958; *Shen and Meyer*, 1963; *Hughes*, 1992]. Following *Hibberd and Peregrine* [1979] and *Packwood* [1980], Kobayashi and colleagues [e.g., *Wurjanto and Kobayashi*, 1991] developed a numerical model (Rbreak) based on (6) and (7) that predicts the evolution of normally incident random waves propagating over irregular (in the cross-shore direction) impermeable bathymetry. Dissipation owing to wave breaking in the model (see Appendix) is approximately equal to the theoretical bore dissipation derived from the nonlinear shallow water equations [e.g., *Ritchmyer and Morton*, 1967; *Meyer and Taylor*, 1972]. Rbreak contains many assumptions [*Kobayashi et al.*, 1989; *Raubenheimer et al.*, 1995], as do all existing models for the propagation and run-up of breaking random waves, and the range of conditions for which Rbreak is accurate is unknown [*Kobayashi*, 1987; *Synolakis*, 1987a]. One purpose of the present study is to better establish the applicability of Rbreak to random wave run-up on natural beaches.

Rbreak is initialized at the model seaward boundary (see Appendix) with observations from the most offshore collocated pressure sensor and current meter (Figure 1). For each 68-min data run, the observed time series of pressure and cross-shore current fluctuations used to initialize Rbreak were low-pass filtered to include only long waves ($(kh)^2 << 1$, where $k$ is the wavenumber), consistent with the derivation of (6) and (7). The high-frequency cutoff was 0.18 Hz at both Scripps and San Onofre and the largest $(kh)^2$ at the initial conditions was 0.38. The predicted band-passed ($0.004 < f \leq 0.18$ Hz) run-up and reflection coefficients are not sensitive to the filtering of the initial conditions. The still water depth input to the model was determined from the observed pressure time series every 17 min. Only the final 51 min of each observed and

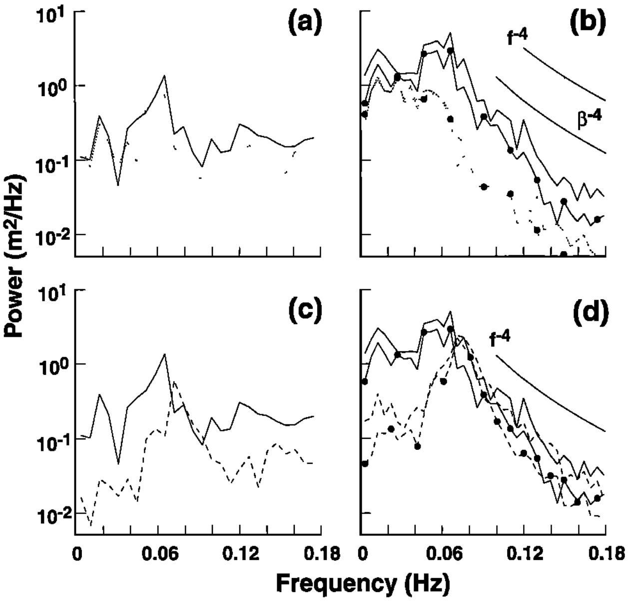


**Figure 2.** Observed spectra at the most offshore sensor, P0 (Figures 2a and 2c), and observed (lines) and predicted (lines with solid circles) spectra at the bottom run-up wire, R05 (Figures 2b and 2d), for three 51-min-long data sets from San Onofre with $H_s = 1.07$ m, $\beta = 0.09$, $\xi_0 = 1.63$ (solid lines); $H_s = 1.07$ m, $\beta = 0.06$, $\xi_0 = 1.14$ (dotted line); $H_s = 0.48$ m, $\beta = 0.09$, $\xi_0 = 2.12$ (dashed line). Smooth solid lines indicate $f^{-4}$ slopes in Figures 2b and 2d and are separated in Figure 2b by a distance proportional to $\beta^4$.

predicted 68-min time series were analyzed to eliminate transients owing to the intial condition of no wave motion. On the basis of previous calibrations and model tests [e.g., *Kobayashi et al.*, 1989; *Cox et al.*, 1992; *Kobayashi and Wurjanto*, 1992; *Raubenheimer et al.*, 1995], a friction coefficient $f_c = 0.015$ and a normalized step size $\Delta x' = 0.01$ (see Appendix) were used for all predictions shown here (the predictions are not sensitive to these values).

## 4. Model-Data Comparisons

Pressure at the initial conditions (P0) and run-up spectra at the lowest wire (R05) are shown in Figure 2 for three selected runs with similar peak frequencies ($\approx$ 0.06 Hz). For the data shown in Figures 2a and 2b the offshore significant wave height is approximately constant and the foreshore slope varies (owing to different tidal stages), whereas for the data shown in Figures 2c and 2d the foreshore slope is approximately constant and the offshore significant wave height varies. Consistent with previous field and laboratory observations (discussed in section 1) and with existing heuristic formulations (2, $\xi_0 < \xi_c$) and (5), run-up energy levels in the sea swell frequency band are saturated (independent of the offshore wave height when the foreshore slope is approximately constant, Figures 2c and 2d), decay approximately as $f^{-4}$ (Figures 2b and 2d), and, for similar offshore wave conditions, increase approximately as $\beta^4$ (Figures 2a and 2b).

For all runs, observed (Figure 3b) and predicted (Figure 3c) R05 run-up spectral levels at frequencies greater than about 0.05 Hz decrease approximately as $f^{-4}$ similar to the three example runs (Figures 2b and 2d). In contrast, the infragravity run-up energy levels are roughly constant with frequency and fall below the $f^{-4}$ levels of the sea swell band. The somewhat arbitrary 0.05-Hz division between infragravity and sea swell frequency bands was selected to be below the offshore spectral peak frequency of all runs (Figure 3a). Since run-up energy at frequencies greater than 0.18 Hz is small (Figure 3b) and may be influenced by the filtering of the model initial conditions or difficulties with the run-up wires (e.g., kelp and see *Holman and Guza* [1984]), all further comparisons to the empirical parameterizations ((2, $\xi_0 < \xi_c$) and (3)) will be made for the sea swell frequency band $0.05 < f \leq 0.18$ Hz. Predicted and observed sea swell significant run-up excursions, $R_s^{ss}$ (based on the run-up variance in the sea swell frequency band), increase with $\beta^2$ as predicted by (2, $\xi_0 < \xi_c$) (Figure 4). Variations in offshore wave steepness (which are much smaller than the variations in foreshore slope in this data set) likely contribute to the scatter about the $\beta^2$ trend (e.g., (2, $\xi_0 < \xi_c$)).

At the lowest wire, $R_s^{ss}/H_s$ is observed and predicted by Rbreak to increase with increasing $\xi_0$ (Figure 5c). Prediction errors are typically less than 20% (Figure 5d). The observed and predicted dependence of $R_s^{ss}$ on $\xi_0$ is somewhat scattered and is approximately equally well described by linear (3) [e.g., *Hunt,* 1959; *Holman and Sallenger,* 1985] and quadratic (e.g., (2, $\xi_0 < \xi_c$) and Figure 4) fits. Linear fits to the present and *Holman*

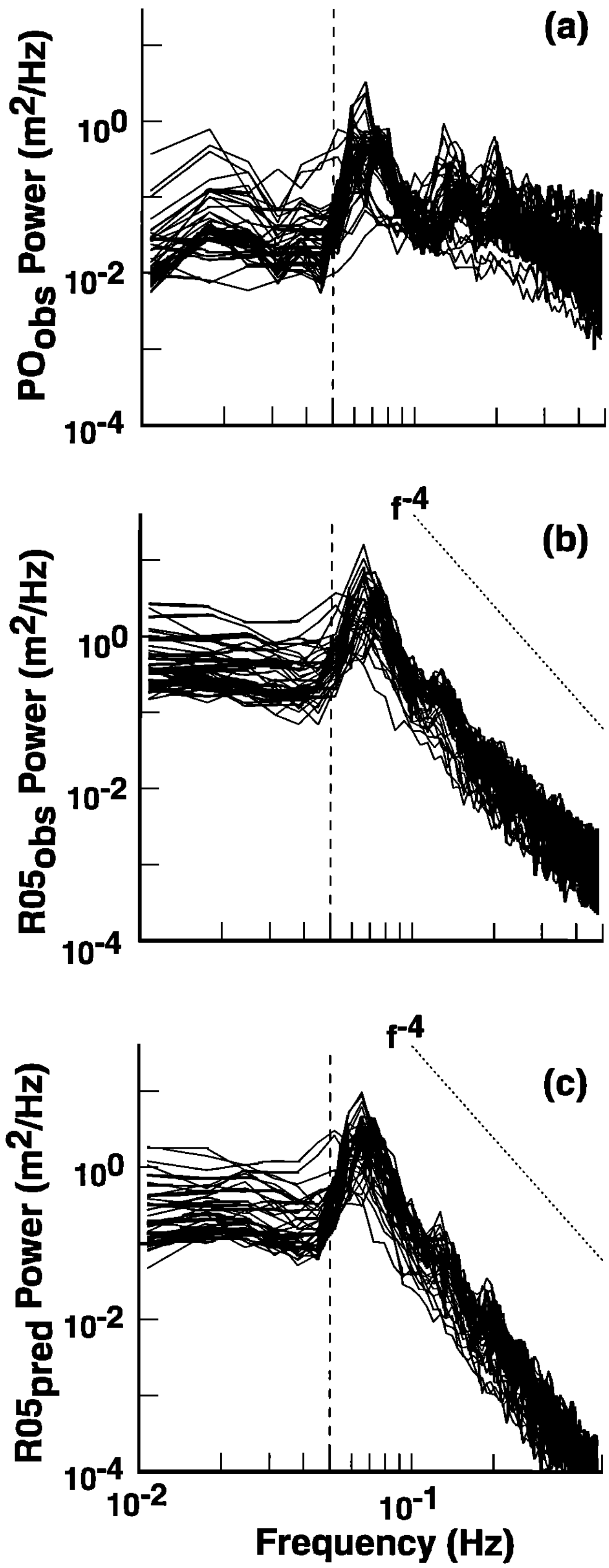


Figure 3. (a) Observed spectra at the model initial conditions (P0) and (b) observed and (c) predicted R05 run-up spectra for all runs. The dotted lines have an $f^{-4}$ slope (e.g., (5)). The vertical dashed lines at 0.05 Hz indicate the division between infragravity and sea swell frequency bands.

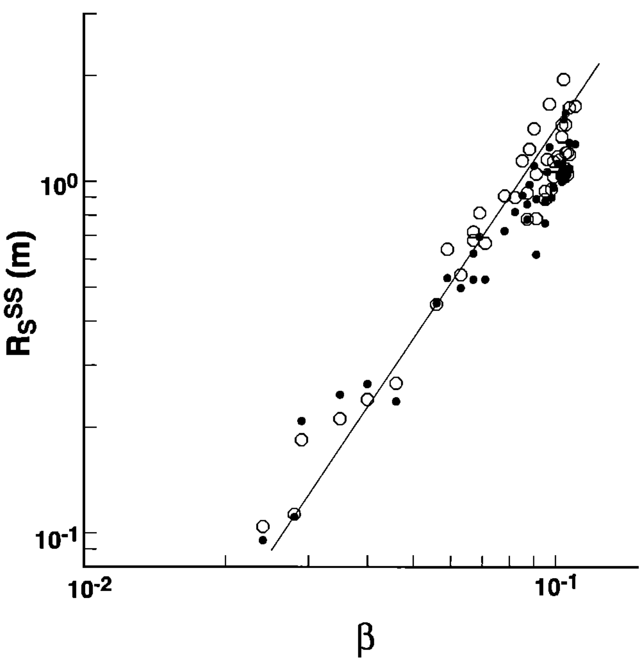


Figure 4. Observed (open circles) and Rbreak predicted (solid circles) sea swell ($0.05 < f \leq 0.18$ Hz) significant run-up excursions, $R_s^{ss}$, at R05 versus foreshore slope, $\beta$. The solid line represents the empirical $\beta^2$ dependence (2, $\xi_0 < \xi_c$).

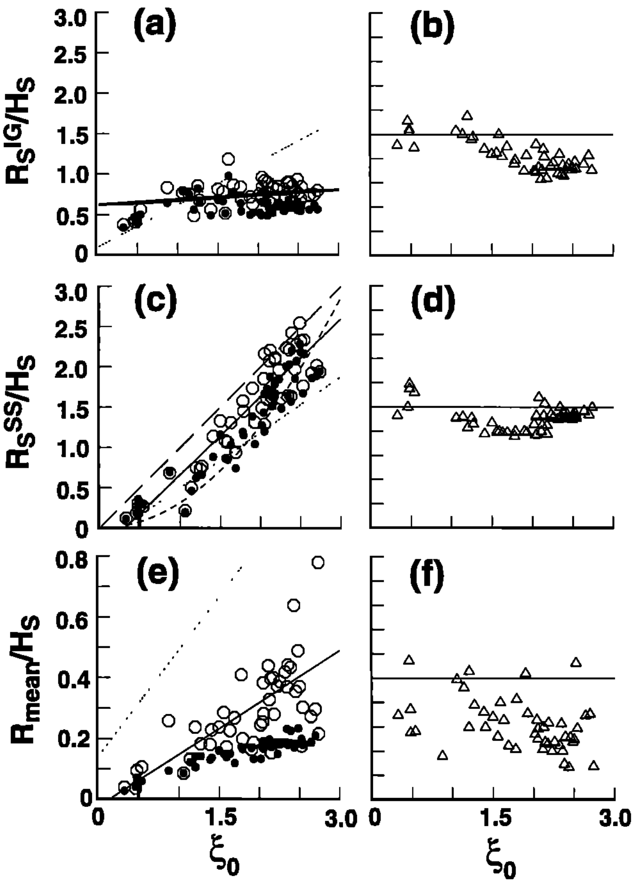


**Figure 5.** For all 49 data runs, observed (open circles) and predicted (solid circles) (a) normalized infragravity ($0.004 \leq f \leq 0.05$ Hz) run-up excursion and (b) prediction error (triangles, $(R_{\text{pred}} - R_{\text{obs}})/R_{\text{obs}}$), (c) normalized sea swell ($0.05 < f \leq 0.18$ Hz) run-up excursion and (d) prediction error, and (e) normalized mean vertical run-up superelevation and (f) prediction error versus Irribarren number, $\xi_0$. Least squares linear fits are shown for the present observations (solid lines) and the infragravity, sea swell, and mean high tide run-up superelevations reported by *Holman and Sallenger* [1985] (dotted lines). In Figure 5c, the short dashed line represents the Miche hypothesis ((2, $\xi_0 < \xi_c$) and the long dashed line represents the "Hunt Formula" (3). The linear fits (and correlations, r) to the present data are $R_s^{IG}/H_s = 0.65 + 0.07\xi_0$, r = 0.26 (Figure 5a); $R_s^{ss}/H_s$ = -0.31 + 0.97$\xi_0$, r = 0.75 (Figure 5c); and $R_v^{\text{mean}}/H_s$ = -0.02 + 0.17$\xi_0$, r = 0.73 (Figure 5e), where $R_s^{ss}$ is the significant run-up height in the sea swell frequency band, $R_s^{IG}$ is the significant run-up height in the infragravity band, and $R_v^{\text{mean}}$ is the mean run-up superelevation.

*and Sallenger* [1985] observations are qualitatively similar (compare solid and dotted lines in Figure 5c). The Hunt Formula (3) gives an approximate upper bound to the observed and predicted normalized sea swell run-up and well describes the total normalized run-up (e.g., $R_{tot}/H_s = \sqrt{(R_s^{ss}/H_s)^2 + (R_s^{IG}/H_s)^2}$) (not shown). (Note that all formulas based on $\xi_0$ are sensitive to the definitions of $H_0$, $L_0$, and $\beta$.)

The observed normalized significant infragravity run-up at the lowest wire, $R_s^{IG}/H_s$ (based on the run-up variance in the infragravity frequency band), is nearly constant, independent of $\xi_0$, corresponding to an approximately linear relationship between $R_s^{IG}$ and $H_s$ (Figure 5a). The 0.65 constant of proportionality is similar to the 0.71 value reported by *Guza and Thornton* [1982] based on observations acquired within 50 km of the present experiment sites. The observed and predicted linear relationship between $R_s^{IG}$ and $H_s$ is (perhaps coincidentally) similar to that observed for solitary waves on planar beaches (e.g., $R \propto H^{5/4}$) [*Synolakis,* 1987b]. Infragravity wave heights observed at many locations on the continental shelf (in depths 10-30 m) are also linearly related to sea swell heights. However, there is considerable variation in the constant of proportionality between sites in the same water depth, but on shelves with different widths [*Herbers et al.,* 1995]. Offshore infragravity energy levels may also depend on features of the surf zone bathymetry such as sand bars and low-tide terraces [*Okihiro and Guza,* 1995]. These studies suggest that the functional dependence of infragravity run-up on $\xi_0$ may be site specific and that generalizations of the present observed dependence of infragravity run-up on $\xi_0$ may not be appropriate. For instance, video run-up observations acquired on a North Carolina beach bordered by a broad ($\approx$ 100 km) shelf [*Holman and Sallenger,* 1985] show a different dependence on $\xi_0$ than the present observations, acquired on Southern California beaches bordered by a narrow ($\approx$ 10 km) shelf (see Figure 5a). (Instrumental differences may also play a role.) Although the parametric fits of the present data to $\xi_0$ differ in detail from those of *Holman and Sallenger* [1985], the overall results are qualitatively similar. In both data sets, sea swell excursions dominate the observed near-bed run-up motions for $\xi_0$ greater than about 1.5 (e.g., compare Figures 5a and 5c), whereas infragravity excursions dominate the run-up for smaller $\xi_0$. The errors in the Rbreak predictions of $R_s^{IG}$ are less than 40% (Figure 5b). Observations and predictions of run-up at the wires higher above the beach show similar trends, although the infragravity run-up is smaller (e.g., Figure 8, discussed below).

Rbreak assumes normal wave incidence. However, previous studies suggest that at infragravity frequencies, obliquely propagating low-mode edge waves may be significant very near the shoreline [e.g., *Oltman-Shay and Guza,* 1987]. Lacking longshore observations, the edge wave mode mix in the present data sets cannot be quantified; however, low-mode edge waves trapped shoreward of the model initial conditions (e.g., mode 0 in Figure 6a) will cause an underprediction of energy near the shoreline. Since all waves are assumed normally incident, low-mode edge waves in the model initial conditions (e.g., mode 1 in Figure 6a) as well as in the run-up will result in prediction errors owing to the difference between the cross-shore amplitude structure of the assumed (normally incident) and observed (edge) waves (e.g., compare mode 1 and leaky amplitude structures in Figure 6a). The cross-shore struc-

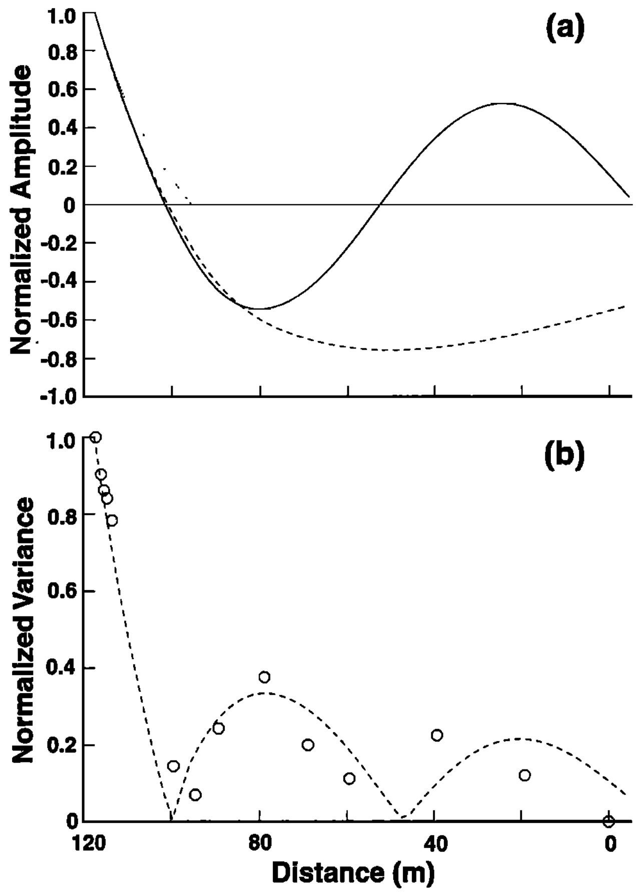


**Figure 6.** (a) Cross-shore variation of sea-surface displacement ($f = 0.045$ Hz) predicted by inviscid linear theory for mode 0 (dotted line) and mode 1 (dashed line) edge waves and leaky waves (solid line) on the measured San Onofre bathymetry. (b) Typical cross-shore distribution of normalized variance error (the difference between the observed and predicted variance divided by the variance error at R05) (circles, for a 51-min run with $H_s = 0.48$ m, $\beta = 0.09$, and $\xi_0 = 2.12$) and variance for a linear combination of mode 0, 1, and 10 edge waves (dashed line) with amplitudes selected to fit approximately the error.

ture of the variance error, the difference between the observed and Rbreak predicted infragravity variance, is qualitatively consistent with low-mode edge waves in the observations. Figure 6 shows the variance for a combination of low-mode edge and normally incident standing waves (based on linear theory) and errors at 0.045 Hz for an example run. Although low-mode edge waves contribute to model errors, the observed infragravity run-up excursions are predicted qualitatively well (Figures 5a and 5b and see below). In these observations, infragravity motions are not dominated by low-mode edge waves with cross-shore (between the run-up and the model initial conditions) amplitude structures significantly different from those of leaky waves.

The normalized mean vertical R05 run-up superelevation (e.g., wave "setup" measured by run-up wires) above the mean water level (MWL) (measured at P0) is observed and predicted by Rbreak to increase approximately linearly with increasing $\xi_0$ (Figure 5e). *Holman and Sallenger* [1985] observed a similar, but steeper, trend at high and mid tides (compare solid and dotted lines in Figure 5e). The differences could be owing to differences in measurement technique since video estimates of mean run-up are considerably larger than estimates from wires 5 cm above the bed [*Holland et al.*, 1995, Figure 2a]. In contrast to the observations of *Holman and Sallenger* [1985], the tidal stage does not affect the present observed mean run-up superelevation. Rbreak predicts a weaker increase in normalized mean superelevation with increasing $\xi_0$ than observed (Figure 5e), and thus Rbreak typically underpredicts the observed superelevation of the mean run-up (Figure 5f).

Observed and predicted squared reflection coefficients, $Re^2$, at San Onofre at P60 were crudely estimated using collocated sea surface elevation and cross-shore current fluctuations [*Raubenheimer et al.*, 1995]. At the model seaward boundary (P0), the observed and predicted $Re^2$ are equal and determined by the observed sea surface elevation and cross-shore velocity time series used to initialize the model. Similar to $Re^2$ at P0 (not shown), surf zone $Re^2$ (based on the band-passed seaward and shoreward propagating energies) are high ($\approx 1.0$) at low infragravity frequencies ($0.004 < f \leq 0.03$ Hz), variable at high infragravity frequencies ($0.03 < f \leq 0.05$ Hz), and relatively small (usually $< 0.4$) at sea swell frequencies (Figure 7a). The increase in sea swell $Re^2$ with increasing $\xi_0$ (Figure 7b) is qualitatively consistent with Miche's empirical reflection formula (4). Reflection coefficients in the surf zone typically increase in the onshore direction, consistent with strong dissipation of shoreward propagating energy relative to seaward propagating energy. For example, observed and predicted sea swell $Re^2$ (Figure 7c) are larger at P60 than at P0 (at the model seaward boundary at San Onofre), except at low $\xi_0$ where $Re^2$ are very small (Figure 7b) and errors in both observed and predicted $Re^2$ are large relative to $Re^2$ itself.

As previously observed [*Holman and Guza,* 1984; *Holland et al.,* 1995], thin run-up tongues cause a sensitivity to wire elevation (e.g., bottom wires measure larger total run-up excursions and mean superelevations than top wires), and run-up measured at different elevations can be used to infer the shape of the run-up tongue [*Raubenheimer et al.,* 1995]. Ratios between measurements at different wires are shown for all five wires for three example runs in Figure 8 and for top and bottom wires for all runs in Figure 9. The ratio of infragravity run-up excursions measured by the top and bottom wires is predicted and observed to be approximately independent of $\xi_0$ and near unity (Figures 8a and 9a). Errors in the predicted ratio are less than about 0.3 (Figure 9b). Predicted and observed normalized sea swell and vertical mean run-up superelevation are more sensitive to wire elevation (Figures 8b, 8c, 9c, and 9e). As previously reported [*Holland et al.,* 1995; *Raubenheimer et al.,* 1995], on the low-sloped Scripps Beach where sea swell run-up excursions are small (Figure 5c, $\xi_0 < 0.6$), significant sea swell excursions are sometimes larger at R25 than at R05 (ratios > 1.0), possibly owing to dissipation of sea swell energy in the run-up (Figure 9c, $\xi_0 < 0.6$). However, on the steeper San Onofre Beach (where $\xi_0 > 0.6$) the ratio of sea swell run-up excursions measured by R25 to those measured by R05 is generally about 0.5 (Figure 9c). That is, owing to thin run-up tongues, sea swell excursions measured by the upper wire are about half those measured by the lowest wire. The model tends to underpredict the ratios, with predictions and observations typically differing by less than 0.2 (Figure 9d). Rbreak estimates run-up oscillations at each wire with comparable accuracy (not shown). Observed ratios between vertical mean run-up superelevation measured by R25 and R05 (Figure 9e) are scattered from about 1.0 (corresponding to a horizontal mean sea surface in the swash zone) to less than zero (corresponding to a mean run-up at R25 that is below the MWL measured at P0). Predicted differences increase slightly with increasing $\xi_0$ from about zero to about 0.5. The reasons for the large errors in mean run-up superelevation (Figures 9e and 9f) are unknown.

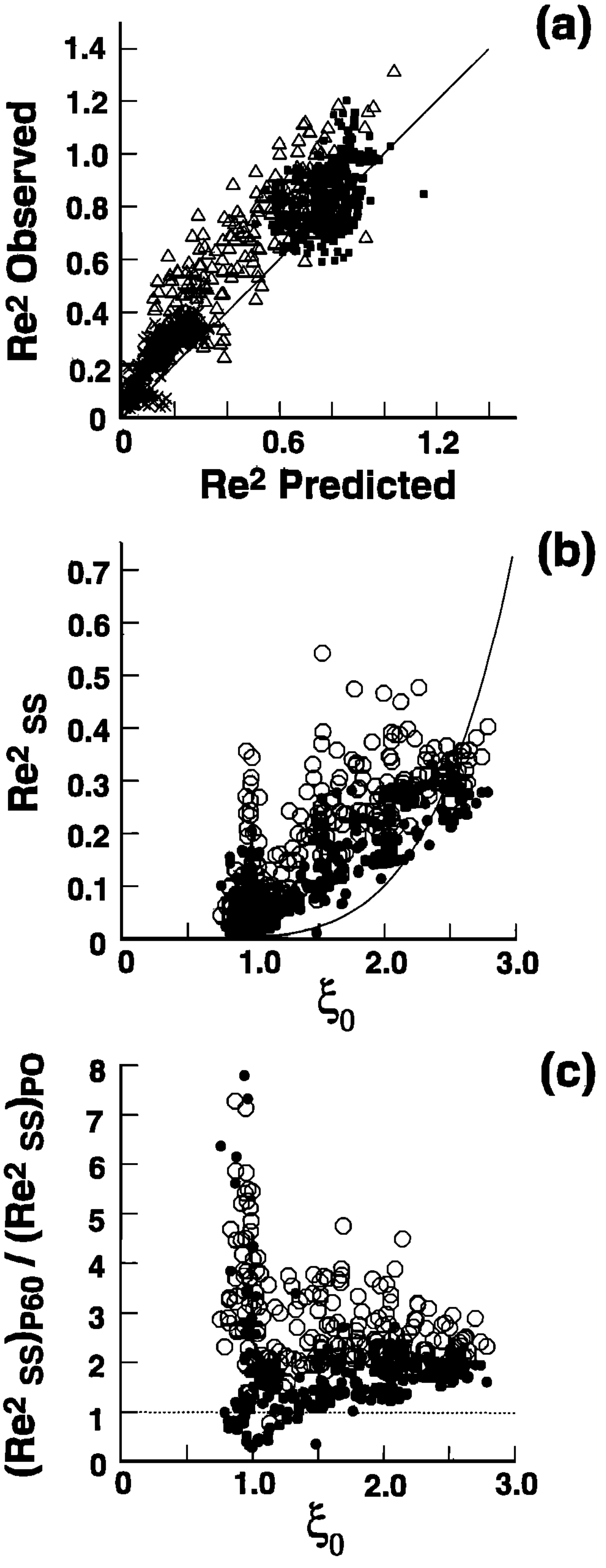


The small vertical separation (20 cm) between top and bottom wires may result in large (up to about 20 m) horizontal separation of measured mean run-up locations. Therefore there may be significant frequency dependent phase differences observed between run-up time series measured at different wires (Figure 10) [*Holland et al.*, 1995; *Raubenheimer et al.*, 1995], similar to the phase difference observed between sea surface elevation time series measured at fixed horizontal locations separated by $O(20$ m$)$. Standing waves result in phase differences of either 0° or 180° (e.g., simultaneous run-up on the bottom wire and run-down on the upper wires [*Raubenheimer et al.*, 1995]), whereas approximately nondispersive progressive waves (e.g., run-up owing to the collapse of shoreward propagating bores) result in phase differences which increase approximately linearly with frequency. Consistent with high reflection coefficients at P60 (Figure 7a), at low infragravity frequencies ($f \leq 0.04$ Hz) the run-up motions are standing and the observed zero phase lag between wires is well predicted by both inviscid (e.g., nonbreaking) linear theory [e.g., *Holland et al.*, 1995] and Rbreak (Figure 10). The phase (relative to the bottom run-up wire) and amplitude structure across the surf zone (not shown) is also consistent with linear free waves at low infragravity frequencies (see also *Raubenheimer et al.* [1995]). At high $\xi_0$ (Figure 10, dashed lines), standing wave energy in the run-up may be significant at swell frequencies (e.g., 0.08 Hz), consistent with relatively high $Re^2$ (Figure 7b). However at lower $\xi_0$ (Figure 10, solid lines), consistent with surf zone $Re^2$ which are typically much less than 1.0, shoreward progressive waves at swell frequencies (e.g., 0.08 Hz) may distort the phase differences

Figure 7. (a) Predicted versus observed squared reflection coefficients, $Re^2$, at P60 for $0.004 \leq f \leq 0.03$ Hz (solid squares), $0.03 < f \leq 0.05$ Hz (triangles), and $0.05 < f \leq 0.18$ Hz (crosses). The solid 45° line represents perfect agreement between predictions and observations. ($Re^2$ is based on the ratio of seaward to shoreward propagating energy, with the energies integrated over the indicated bands). (b) Predicted (solid circles) and observed (open circles) sea swell ($0.05 < f \leq 0.18$ Hz) reflection coefficients versus $\xi_0$. The solid curve represents (4). (c) Predicted (solid circles) and observed (open circles) ratio of sea swell $Re^2$ at P60 to that at P0 versus $\xi_0$. Points above the dotted line represent increasing reflection coefficients in the onshore direction.

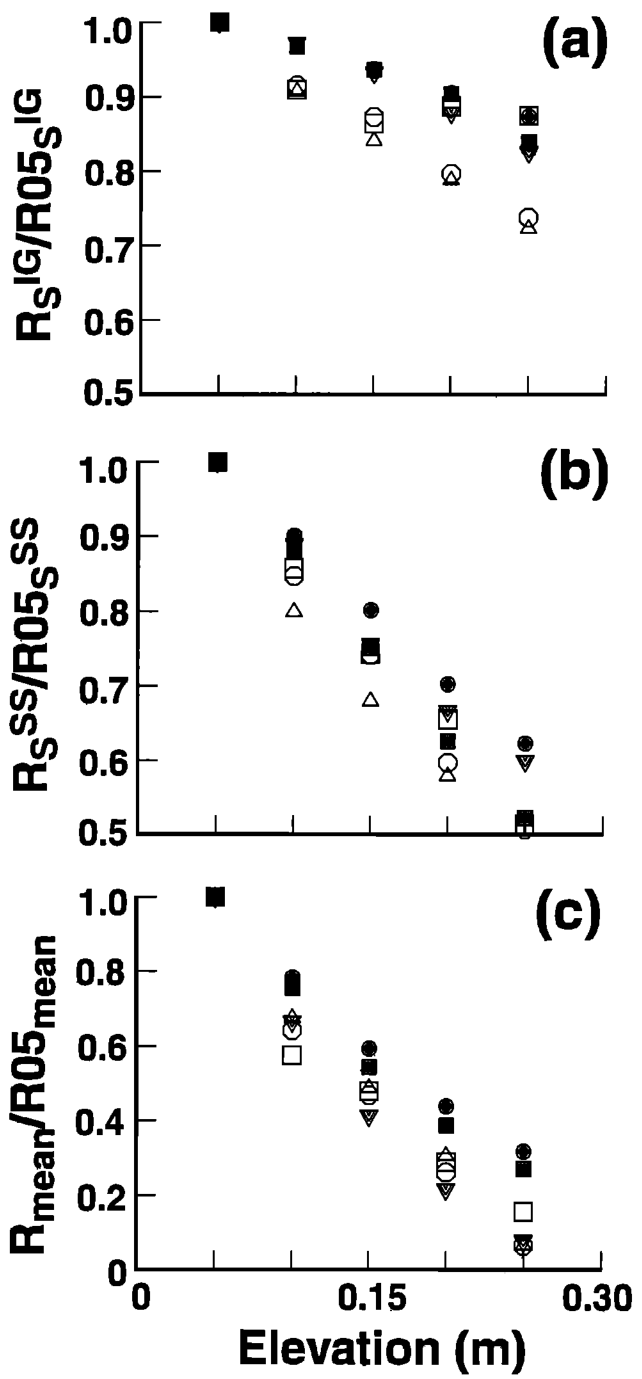


**Figure 8.** Observed (open symbols) and predicted (solid symbols) normalized (by observations and predictions, respectively, at the bottom wire) (a) infragravity ($0.004 \le f \le 0.05$ Hz) and (b) sea swell ($0.05 < f \le 0.18$ Hz) run-up excursions ($R_s^{IG}$ and $R_s^{ss}$ in Figures 8a and 8b, respectively) and (c) mean vertical run-up superelevation, $R_{\text{mean}}$, versus wire elevation. Three representative 51-min runs are shown: $H_s = 1.07$ m, $\beta = 0.06$, $\xi_0 = 1.14$ (triangles); $H_s = 1.07$ m, $\beta = 0.09$, $\xi_0 = 1.63$ (circles); and $H_s = 0.48$ m, $\beta = 0.09$, $\xi_0 = 2.12$ (squares).

from the standing wave values and the observed and Rbreak predicted phases diverge from inviscid linear theory. Phase lag prediction errors of Rbreak are usually less than 25°(not shown).

## 5. Discussion

Predicted and observed band-passed ($0.004 < f \le 0.18$ Hz) horizontal run-up locations at 5 and 25 cm above the bed are shown in Figure 11a for a typical uprush and downrush. The Rbreak-predicted depth-averaged velocities at six locations and the shape of the run-up are shown at four times during this 14-s period (Figures 11b-11e). Previous studies have shown that the depth-averaged swash velocities are accurately predicted by Rbreak for laboratory monochromatic waves [*van der Meer and Breteler*, 1990]. The good agreement between predicted and observed run-up in the present study suggests that random wave swash velocities may also be accurately modeled.

Similar to previous predictions and observations of solitary [*Synolakis*, 1987b; *Svendsen and Grilli*, 1990] and random wave run-up [*Raubenheimer et al.*, 1995], a bore moves up the beach (Figure 11b), collapses to form a thin concave tongue (Figures 11c and 11d), and retains this shape during the run-down (Figure 11e). The predicted thinning of the run-up tongue results from mass conservation and velocities which are largest at the run-up tip (Figures 11c and 11d). Since run-up wires measure the changing location of a particular depth of

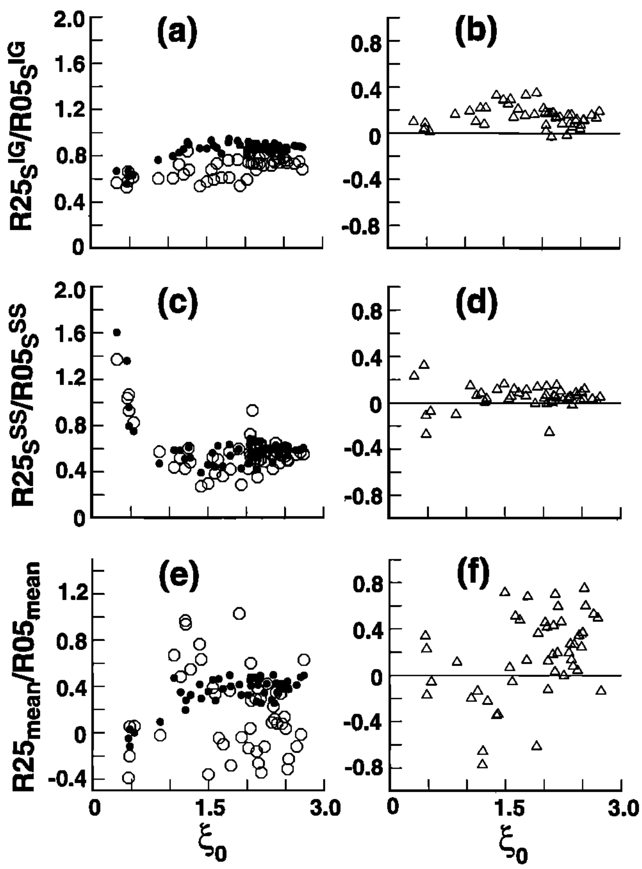


**Figure 9.** Predicted (solid circles) and observed (open circles) ratio between run-up on top (R25) and bottom (R05) wires versus $\xi_0$ for infragravity and sea swell frequency band (Figures 9a and 9c, respectively) excursions and mean vertical run-up superelevation (Figure 9e). Figures 9b, 9d, and 9f show the prediction errors, $[(R25_{\text{pred}}/R05_{\text{pred}}) - (R25_{\text{obs}}/R05_{\text{obs}})]$.

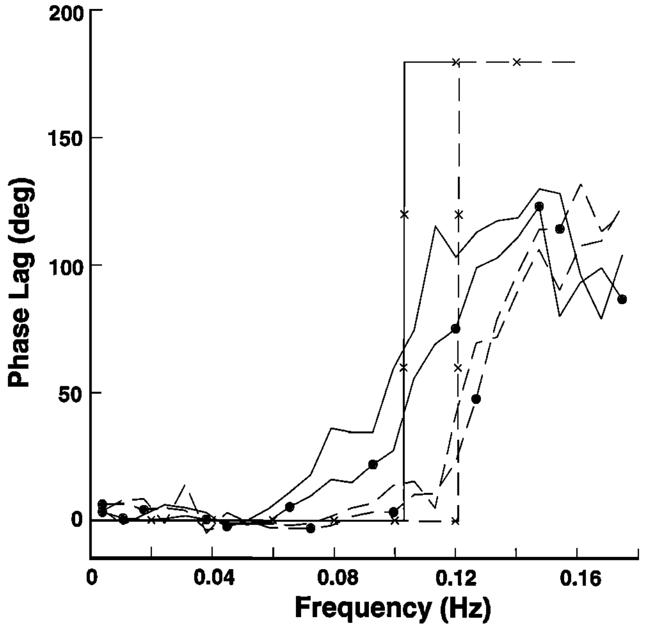


**Figure 10.** Phase lags observed (solid and dashed lines), predicted with Rbreak (lines with solid circles) and predicted with linear standing wave theory (lines with crosses) between run-up at 25 and 5 cm above the bed versus frequency for two data runs: $H_s$ = 0.53 m, $\beta$ = 0.11, $\xi_0$ = 2.74 (dashed lines) and $H_s$ = 1.07 m, $\beta$ = 0.09, $\xi_0$ = 1.63 (solid lines).

water rather than sea surface elevation fluctuations ($\eta$) as in the nonlinear shallow water equations, fluid velocities are not simply related to run-up observations. In fact, while the flow is directed onshore, the thinning of the run-up tongue may result in simultaneous measurement of "run-down" by the upper wire and "run-up" by the bottom wire (e.g., Figure 11a at t = 4 s and Figure 11c). In other words, although run-up measured a few centimeters above the bed (e.g., by the bottom wire) may be closely related to the depth-averaged water velocity near the run-up tip, the measurements 25 cm above the bed (by the upper wire) cannot be used to infer even the sign of the fluid velocities within the run-up tongue.

## 6. Conclusions

Numerical model predictions of run-up based on the one-dimensional depth-averaged nonlinear shallow water equations agree well with both heuristic models and observations with vertically stacked run-up wires. Semiempirical saturation formulations are consistent with numerical model predictions and observations of sea swell run-up excursions and reflection (Figures 2-4, 5c, 5d, and 7b). The relative amount of reflected energy at sea swell frequencies is observed and predicted by the model to increase both with increasing Irribarren number (Figures 7b and 10) and decreasing distance from shore (Figure 7c). At infragravity frequencies, run-up excursions are observed to be unsaturated (e.g., to increase with increasing offshore wave height, Figure 5a), and the numerical model accurately predicts the dominance of waves standing in the cross shore (Figures 7a and 10). Thin concave run-up tongues cause a sensitivity of measured run-up excursions and means to sensor elevation above the bed and phase lags between measurements at different elevations (Figures 8-10).

## Appendix: Model Revision and Dissipation

At the seaward boundary, Rbreak requires time series of the cross-shore velocity $u(0,t)$ and the total water depth,

$$h(0,t) = d + \eta(0,t) = d + \eta_i(t) + \eta_r(t) \qquad \text{(A1)}$$

where $d$ is the still water depth and $\eta_i(t)$ and $\eta_r(t)$ are the shoreward and seaward propagating wave fields, respectively. In previous studies, $d$ was calculated from observations, $\eta_i(t)$ was estimated using observed time series of either the sea surface elevation at several locations [e.g., *Kobayashi et al.,* 1990] or collocated sea surface elevation and cross-shore velocity measurements [e.g., *Raubenheimer et al.,* 1995], and $\eta_r(t)$ was approximated using the characteristic equations (assuming subcritical flow conditions and negligible friction) and linear wave theory [*Kobayashi et al.,* 1989; *Wurjanto and Kobayashi,* 1991]. Previous studies have shown that $\eta_r(t)$ was approximated at least qualitatively well [*Kobayashi et al.,* 1990; *Kobayashi and Raichle,* 1994; *Raubenheimer et al.,* 1995]. The time series of the cross-shore velocity was also calculated from the characteristic equations.

In this study the model has been revised and is initialized directly with observations of $d$, $\eta(0,t)$ and $u(0,t)$, eliminating the linear and characteristic approximations. This method forces the predicted and observed frequency-dependent reflection coefficients $Re^2$ to be equal at the seaward boundary. Run-up variances predicted with the original and revised models differ by less than 15%.

Wave dissipation is included in the model both by the quadratic bottom friction and bore dissipation [e.g., *Stoker,* 1947]. Previous model calibrations have shown that run-up predictions are not sensitive to friction coefficients in the range $0.01 \leq f_c \leq 0.05$ [*Cox et al.,* 1992; *Raubenheimer et al.,* 1995] and, consistent with other run-up models based on the nonlinear shallow water equations [e.g., *Titov and Synolakis,* 1995], total dissipation is dominated by wave breaking [*Kobayashi and Wurjanto,* 1992]. The nonlinear shallow water equations (6) and (7) predict that unbroken waves will steepen within a few wavelengths forming shocks (or bores) [e.g., *Meyer and Taylor,* 1972]. Here the bore dissipation is modeled by using a bore-capturing Lax-Wendroff numerical scheme [*Lax and Wendroff,* 1960]. The theoretical and predicted dissipation are approximately equal so long as the bore front is nearly vertical and covers only a relatively small distance [e.g., *Ritchmyer and Morton,* 1967; *Meyer and Taylor,* 1972].

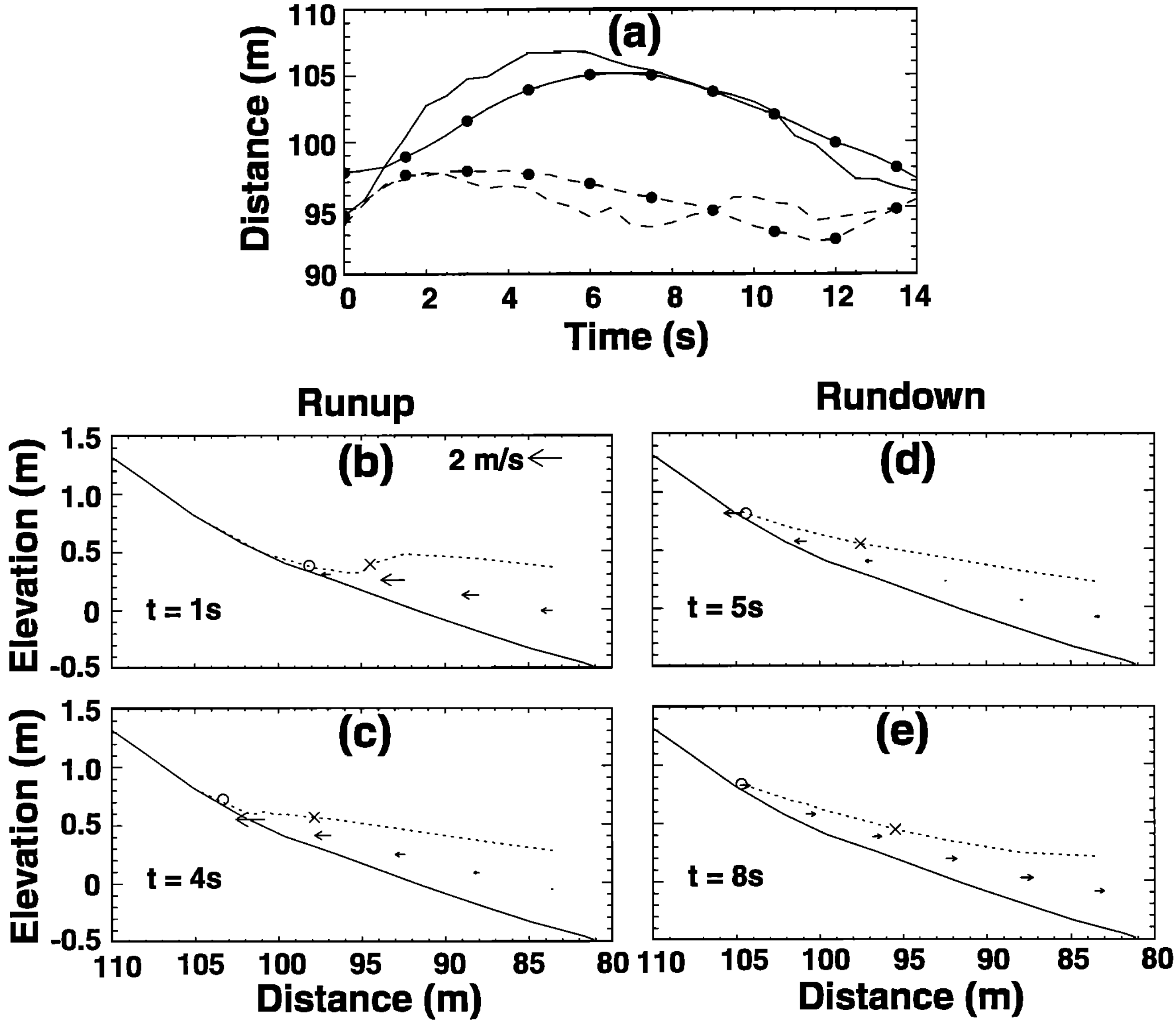


**Figure 11.** (a) Observed (lines) and predicted (lines with solid circles) run-up at 5 cm (solid lines) and 25 cm (dashed lines) above the bed for a single swash event during an example run ($H_s$ = 1.07 m, $\beta = 0.06, \xi_0 = 1.14$) versus time. The predicted swash zone sea surface elevation (dotted lines), locations of run-up measured by R25 (crosses) and R05 (open circles), and velocities at six locations across the swash zone (arrows) are shown for (b) t = 1 s, (c) $t$ = 4 s, (d) $t$ = 5 s, and (e) $t$ = 8 s. (Velocities are not shown for locations that are not submerged.) The scale of the velocity vectors is shown in the upper right corner of Figure 11b.

Since the Lax-Wendroff method spreads the bore front across a few horizontal grid points, the normalized step size, $\Delta x'$, must be small, $\Delta x' = (\Delta x / T\sqrt{gH}) << 1$, where $\Delta x$ is the dimensional step size. Previous results showed that predicted run-up time series, variance, and skewness do not significantly vary for a plausible range of $\Delta x'$ [*Raubenheimer et al.*, 1995]. Long wavelength (e.g., infragravity) waves are not necessarily predicted to form shocks (and dissipate) within the model domain, whereas shorter wavelength sea swell waves are nearly always predicted to break, as is observed.

**Acknowledgments.** This research was supported by ONR (Coastal Dynamics, Waves in the Ocean BAA, and AASERT graduate student support) and NSF. Staff from the Center for Coastal Studies deployed and maintained the nearshore instruments. Offshore wave information was provided by the Coastal Data Information Program. The cooperation of the staffs at the Orange Coast Division of the State of California Department of Parks and Recreation and San Onofre State Park is gratefully acknowledged. Steve Elgar and Nobu Kobayashi are thanked for their helpful comments and suggestions.

## References

Ahrens, J. P., Irregular wave runup on smooth slopes, *Coastal Eng. Tech. Aid 81-17*, U.S. Army Eng. Coastal Eng. Res. Center, Ft. Belvoir, Va., 1981.

Battjes, J. A., Surf similarity, paper presented at the 14th International Conference on Coastal Engineering, Am. Soc. of Civ. Eng., Copenhagen, Denmark, 1974.

Carrier, G. F., and H. P. Greenspan, Water waves of finite amplitude on a sloping beach, *J. Fluid Mech., 4*, 97-109, 1958.

Cox, D. T., N. Kobayashi, and A. Wurjanto, Irregular wave transformation processes in surf and swash zones, paper presented at the 23rd International Conference on Coastal Engineering, Am. Soc. of Civ. Eng., Venice, Italy, 1992.

Elgar, S., T. H. C. Herbers, and R. T. Guza, Reflection of ocean surface gravity waves from a natural beach, *J. Phys. Oceanogr., 24*, 1503-1522, 1994.

Guza, R. T., and A. J. Bowen, Resonant interactions for waves breaking on a beach, paper presented at the 15th International Conference on Coastal Engineering, Am. Soc. of Civ. Eng., Honolulu, Hawaii, 1976.

Guza, R. T., and E. B. Thornton, Swash oscillations on a natural beach, *J. Geophys. Res., 87*, 483-491, 1982.

Guza, R. T. , E. B. Thornton, and R.A. Holman, Swash on steep and shallow beaches, paper presented at the 19th International Conference on Coastal Engineering, Am. Soc. of Civ. Eng., Houston, Tex., 1984.

Herbers, T. H. C., S. Elgar, R. T. Guza, and W. C. O'Reilly, Infragravity-frequency (0.005-0.05 Hz) motions on the shelf, II, Free waves, *J. Phys. Oceanogr., 25*, 1063-1079, 1995.

Hibberd, S., and D. H. Peregrine, Surf and run-up on a beach, *J. Fluid Mech., 95*, 323-345, 1979.

Holland, K. T., B. Raubenheimer, R. T. Guza, and R. A. Holman, Runup kinematics on a natural beach, *J. Geophys. Res., 100*, 4985-4993, 1995.

Holman, R. A., and R. T. Guza, Measuring run-up on a natural beach, *Coastal Eng., 8*, 129-140, 1984.

Holman, R. A., and A. H. Sallenger, Setup and swash on a natural beach, *J. Geophys. Res., 90*, 945-953, 1985.

Hughes, M. G., Application of a non-linear shallow water theory to swash following bore collapse on a sandy beach, *J. Coastal Res., 8*, 562-578, 1992.

Hunt, I. A., Jr., Design of seawalls and breakwaters, *J. Waterw. Harbors Div., 85*, 123-152, 1959.

Huntley, D., R. T. Guza, and A. J. Bowen, A universal form for shoreline run-up spectra?, *J. Geophys. Res., 82*, 2577-2581, 1977.

Kobayashi, N., Closure of wave reflection and run-up on rough slopes, *J. Waterw. Port Coastal Ocean Eng., 113*, 143-148, 1987.

Kobayashi, N., and A. W. Raichle, Irregular wave overtopping of revetments in surf zones, *J. Waterw. Port Coastal Ocean Eng., 120*, 56-73, 1994.

Kobayashi, N., and K. D. Watson, Wave reflection and runup on smooth slopes, paper presented at the Conference on Coastal Hydrodynamics, Am. Soc. of Civ. Eng., 1987.

Kobayashi, N., and A. Wurjanto, Irregular wave setup and run-up on beaches, *J. Waterw. Port Coastal Ocean Eng., 118*, 368-386, 1992.

Kobayashi, N., A. K. Otta, and I. Roy, Wave reflection and run-up on rough slopes, *J. Waterw. Port Coastal Ocean Eng., 113*, 282-298, 1987.

Kobayashi, N., M. S. Strzelecki, and A. Wurjanto, Swash oscillation and resulting sediment movement, paper presented at the 21st International Conference on Coastal Engineering, Am. Soc. of Civ. Eng., Malaga, Spain, 1988.

Kobayashi, N., G. S. DeSilva, and K. D. Watson, Wave transformation and swash oscillation on gentle and steep slopes, *J. Geophys. Res., 94*, 951-966, 1989.

Kobayashi, N., D. T. Cox, and A. Wurjanto, Irregular wave reflection and run-up on rough impermeable slopes, *J. Waterw. Port Coastal Ocean Eng., 116*, 708-728, 1990.

Lax, P., and B. Wendroff, Systems of conservation laws, *Commun. Pure Appl. Math, 13*, 217-237, 1960.

Mase, H., Spectral characteristics of random wave run-up, *Coastal Eng., 12*, 175-189, 1988.

Meyer, R. E., and A. D. Taylor, Runup on beaches, in *Waves on Beaches and Resulting Sediment Transport*, edited by R. E. Meyer, pp. 357-411, Academic, San Diego, Calif., 1972.

Miche, R., Le pouvoir réfléchissant des ouvrages maritimes exposés à l'action de la houle, *Ann. Ponts Chaussees, 121*, 285-319, 1951.

Mizugushi, M., Swash on a natural beach, paper presented at the 19th International Conference on Coastal Engineering, Am. Soc. of Civ. Eng., Houston, Tex., 1984.

Moraes, C. de C., Experiments of wave reflection on impermeable slopes, paper presented at the 12th International Conference on Coastal Engineering, Am. Soc. of Civ. Eng., Washington, DC, 1970.

Okihiro, M., and R. T. Guza, Infragravity energy modulation by tides, *J. Geophys. Res., 100*, 16,143-16,148, 1995.

Oltman-Shay, J., and R. T. Guza, Infragravity edge wave observations on two California beaches, *J. Phys. Oceanogr., 17*, 644-663, 1987.

Packwood, A. R., Surf and run-up on beaches, Ph.D. thesis, 178 pp., School of Math., Univ. of Bristol, Bristol, England, 1980.

Raubenheimer, B., R. T. Guza, Steve Elgar, and N. Kobayashi, Swash on a gently sloping beach, *J. Geophys. Res., 100*, 8751-8760, 1995.

Ritchmyer, R. D., and K. W. Morton, *Difference Methods for Initial-Value Problems*, 2nd ed., 354 pp., Wiley-Interscience, New York, 1967.

Sawaragi, T., and K. Iwata, A nonlinear model of irregular wave run-up height and period distributions on gentle slopes, paper presented at the 19th International Conference on Coastal Engineering, Am. Soc. of Civ. Eng., Houston, Tex., 1984.

Shen, M. C., and R. E. Meyer, Climb of a bore on a beach, 3, Runup, *J. Fluid Mech., 74*, 685-694, 1963.

Stoker, J. J., Water Waves, Wiley Interscience, New York, 1947.

Suhayda, J. N., Standing waves on beaches, *J. Geophys. Res., 79*, 3065-3071, 1974.

Svendsen, I. A., and S. T. Grilli, Nonlinear waves on steep slopes, *J. Coastal Res., 7*, 185-202, 1990.

Synolakis, C. E., Discussion of wave reflection and run-up on rough slopes, *J. Waterw. Port Coastal Ocean Eng., 113*, 139-143, 1987a.

Synolakis, C. E., The run-up of solitary waves, *J. Fluid Mech., 185*, 523-545, 1987b.

Tatavarti, V., D. Huntley, and A. J. Bowen, Incoming and seaward going wave interactions on beaches, paper presented at the 21st International Conference on Coastal Engineering, Am. Soc. of Civ. Eng., Malaga, Spain, 1988.

Titov, V. V., and C. E. Synolakis, Modeling of breaking and nonbreaking long-wave evolution and run-up using VTCS-2, *J. Waterw. Port Coastal Ocean Eng., 121*, 308-316, 1995.

van der Meer, J. W., and M. K. Breteler, Measurement and computation of wave induced velocities on a smooth slope, paper presented at the 22nd International Conference on Coastal Engineering, Am. Soc. of Civ. Eng., Delft, Netherlands, 1990.

Van Oorschot, J. H., and K. d'Agremond, The effect of wave energy spectra on wave run-up, paper presented at the 11th International Conference on Coastal Engineering, Am. Soc. of Civ. Eng., London, England, 1968.

Wise, R. A., N. Kobayashi, and A. Wurjanto, Cross-shore sediment transport under irregular waves in surf zones, paper presented at Coastal Sediments '91, Am. Soc. of Civ. Eng., Seattle, Wash., 1991.

Wurjanto, A., and N. Kobayashi, Numerical model for random waves on impermeable coastal structures and beaches, *Res. Rep. CACR-91-05,* Cent. for Appl. Coastal Res., Univ. of Del., Newark, 1991.

R. T. Guza and B. Raubenheimer, Center for Coastal Studies, Scripps Institution of Oceanography, University of California, San Diego, 9500 Gilman Drive, La Jolla, CA 92093-0209. (email: rtg@coast.ucsd.edu; britt@coast.ucsd.edu)

(Received November 16, 1995; revised May 14, 1996; accepted June 14, 1996.)